ELSEVIER

Surface Science 394 (1997) 150–158

surface science

Surface reconstruction of the Ir(110) surface

J. Kuntze, J. Bömermann, T. Rauch, S. Speller, W. Heiland *

FB Physik, Universität Osnabrück, D-49069 Osnabrück, Germany

Received 5 November 1996; accepted for publication 9 July 1997

Abstract

We report a scanning-tunneling-microscopy (STM) study of the Ir(110) surface. Several structures such as the (1×1), (1×3), (1×4) and the $c(2\times2)$ reconstruction have been found under different preparation conditions. These structures have also been investigated with low-energy electron diffraction (LEED). Surface cleanliness was checked with Auger electron spectroscopy (AES).

Keywords: Iridium; Low-index single crystal surfaces; Scanning tunneling microscopy (STM); Surface structure

1. Introduction and experiment

The investigation of fcc(110) surfaces has been of great interest for many years. For Au(110) and Pt(110), it is known that the clean surfaces show a (1×2) missing-row reconstruction [1–7]. For the Ir(110) surface, however, the structure of the clean surface is still a matter of research. Early results favoured a (1×2) missing row reconstruction as for the Au and Pt surfaces [8–10]. Newer studies reported a (1×3) structure [11–15] and a faceted reconstruction [16–18]. The unreconstructed (1×1) and the $c(2\times2)$ reconstruction have been observed by many groups [8,9,13,19,20]. These structures are possibly induced or stabilized by oxygen and/or carbon monoxide adsorption.

In our study, we investigated the various reconstructions with scanning tunneling microscopy (STM), supported by low-energy electron diffraction (LEED) and Auger electron spectroscopy (AES). Surface preparation was performed in the usual manner by sputtering with 500 eV Ar^+ ions, $I\approx5$mA. The angle of incidence of the ions was approximately 60° to the surface. The sputter gas was cleaned by liquid N_2 freezing before entering the ion-source and the sputtering was followed by annealing cycles. The heating was performed with a tantalum filament placed behind the sample holder. Occasionally, oxygen treatments were used to remove residual carbon or to prepare the (1×1) structure.

We used an OMICRON-STM-1 described in detail elsewhere [21]. The STM was placed in a three chamber ultra-high vacuum (UHV) system with transfer and sample handling facilities. The chambers were sealed by gate valves to provide the possibility of preparing and analysing different samples at the same time and to keep preparation and analysing areas strictly separated. With the transfer system, it was possible to investigate a freshly prepared sample within several minutes with STM. In general, STM measurements were performed before LEED or AES measurements to

* Corresponding author. Tel: (+49) 541 969 26 75; fax: (+49) 541 969 26 70; e-mail: wheiland@dosuni.bitnet

0039-6028/97/$17.00
PII S0039-6028(97)00602-X

avoid effects due to the electron beam. After prolonged LEED, RHEED and/or AES studies, we observed deteriorations of the quality of the STM images. The STM itself can also be used as an indicator of local surface cleanliness [22].

The STM piezos were calibrated using the Si(111) surface and its (7×7) reconstruction, as well as the Pt(110) surface. Step heights corresponding to single and double steps were used to calibrate the z-piezo. Because of a slight deviation from the 90° angles of the tripod scanner, an image correction to rectify the axes had to be used. All STM images shown here were taken at room temperature and were not processed, i.e. smoothed, Fourier-filtered, or differentiated, unless explicitly stated.

To prepare the (1×1) structure, it was necessary to heat the surface in an oxygen atmosphere, as reported in earlier work [12,19]. After 1 h of sputtering, the sample was heated to 600 K and then exposed to 10^{-4} Pa oxygen for about 30 min. The sample was then heated for another 15–30 min under UHV conditions (with no oxygen present in the residual gas) before cooling to room-temperature.

In our work, the $c(2\times2)$ structure was not prepared in the usual reported way, i.e. via oxygen or carbon-monoxide adsorption [8,12,20]. Instead, the structure was reproducibly prepared with heating to 700 ± 20 K after sputtering, without any oxygen treatment. Annealing at higher temperatures of $>950\pm20$ K and with a slow cooling rate (1–5 K/min) led to (1×3) and (1×4) reconstructions, as well as the faceted reconstruction, possibly depending on Ca contamination (see below).

2. Results

2.1. (1×1) Structure

The (1×1) structure was prepared via heating the crystal to 600 ± 20 K in 10^{-4} Pa O_2 for about 30 min. The sample was then annealed for another 30 min under UHV conditions to desorb the oxygen. The annealing temperature must not exceed far beyond this range since the (1×1) structure is metastable and different reconstructions occur at higher temperatures (see below). The (1×1) structure can also be prepared by first heating to high temperatures of ≈950 K thus causing reconstructions described below, and then exposing the surface to oxygen at a temperature of ≈600 K.

In Fig. 1, the mesoscopic step structure of the surface can be seen in an overview STM image. Because of the moderate annealing temperature of only 600 K, the surface shows sputter damage, as reported frequently in the literature, e.g. by Michely et al. [23]. Step heights correspond to single or double steps, as can be seen in the height scan shown in Fig. 1. No triple or multiple steps have been observed. On top of the plateaus atomic resolution has been achieved in [001] direction (Fig. 1b). The distance between the $[1\bar{1}0]$ rows is 3.9 ± 0.1 Å, in agreement with the lattice constant of 3.84 Å. The $[1\bar{1}0]$ rows scale and rotate in the correct manner if the image size or scanning direction are varied so artefacts can be excluded. The periodicity along the $[1\bar{1}0]$ rows can only be derived from the LEED pattern (Fig. 2). We note that except for the image shown in Fig. 1b, no image-processing such as smoothing, Fourier-filtering or differentiation was performed on the pictures presented here.

The LEED pattern (Fig. 2) shows sharp spots which indicate a high order within the coherence zone of the electron beam. In some cases, the intensity distribution of the LEED spots was different, i.e. at the same electron energy as shown in the figure, every other spot was less intense, which led to a LEED pattern similar to that of a centered structure. With changing electron energy, however, all spots seen in Fig. 2 could always be observed.

Fig. 3 shows the corresponding AE spectrum. Small amounts of carbon were detected which almost disappear in the differentiated spectrum, and which we show for comparison with standard spectra. Only a structure at 291 eV could be identified, which corresponds to calcium. The Ca concentration in Fig. 3 is approximately 8% (peak-to-peak evaluation with standard sensitivity factors listed in [24]). This Ca contamination could be removed by further sputtering-cycles (inset in

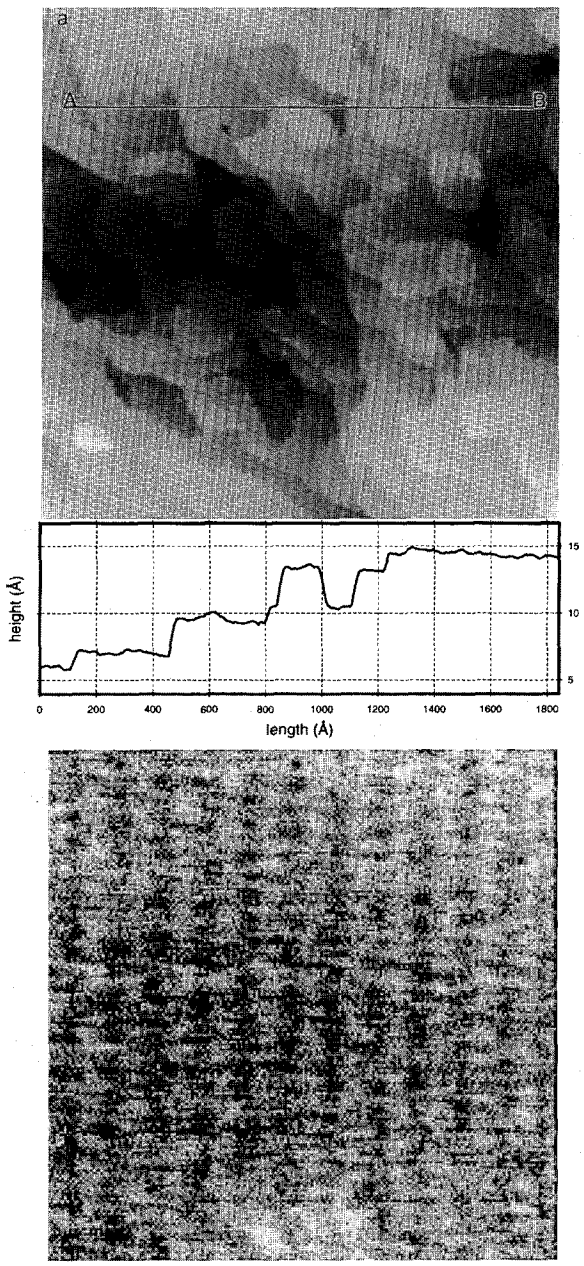

Fig. 1. (a) (2000×2000) Å^2 STM image of the Ir(110)-(1×1) structure ($U_t = -0.28$ V, $I_t = 1.1$ nA). The mesoscopic islands are due to the sputtering. The height scan shows only single- and double steps. (b) (50×50) Å^2 STM image of the Ir(110)-(1×1) structure ($U_t = -0.2$ V, $I_t = 2.0$ nA). The $[1\bar{1}0]$ rows (parallel to the vertical image-axis) are resolved in the [001] direction. For better visibility, the image was slightly Fourier filtered.

Fig. 3). The Ca contamination had no influence on the formation of the (1×1) structure according to STM and LEED, i.e. the results were the same on the clean and the contaminated surface.

2.2. *c(2 × 2) Structure*

The $c(2 \times 2)$ structure was prepared via heating the sample to 700 ± 20 K after sputtering followed by slow cooling to room temperature. The structure was not caused by an overlayer of oxygen, as reported previously [8,9,12,18,19], but represents a reconstruction of the surface. The AE spectrum of the structure was identical to that shown in Fig. 3. The surface exhibits LEED patterns identical for both the Ca-contaminated and the clean surface. We were successful in preparing the structure in the usual reported way via oxygen adsorption, but up to now, no STM data are available. However, the LEED patterns reveal the same symmetry as with the thermally induced structure (prepared without oxygen treatment).

Fig. 4 shows an atomically resolved STM image of the $c(2 \times 2)$ structure. The height scan reveals the theoretically expected period of 4.7 Å, as can be seen in the Fourier transformation of the height scan. Fig. 5 shows an overview STM image where many small terraces can be seen, and which are separated by row-like structures running parallel to the $[1\bar{1}0]$ direction. On each of these terraces, the $c(2 \times 2)$ structure has been found, indicating that there is a considerable amount of this structure present on the surface, in agreement with the LEED pattern (Fig. 6) which reveals the same symmetry regardless of the (lateral) sample position. If the structure would be present only on a small fraction of the surface, the LEED pattern would have changed when varying the sample position. The number of the row-like structures seen in Fig. 5 increases with higher annealing temperatures. This indicates that the $c(2 \times 2)$ structure is metastable and the (1×3), (1×4) and the faceted reconstruction are formed eventually (see below).

2.3. *(1 × 3)/(1 × 4) Structure, faceted reconstruction*

These structures are obtained by heating the sample to 950–1050 K for about 30 min and slow

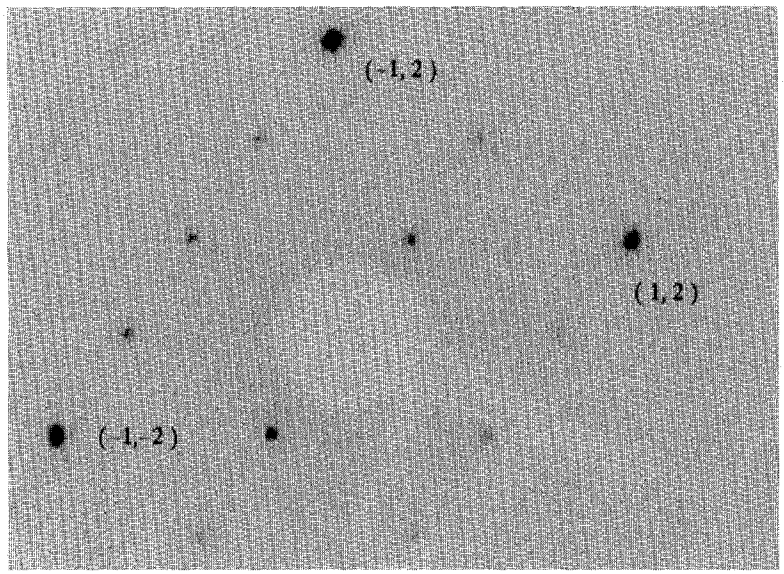

Fig. 2. LEED pattern of the Ir(110)-(1 × 1) structure. The electron energy is 146 eV. Several integral-order spots are indexed.

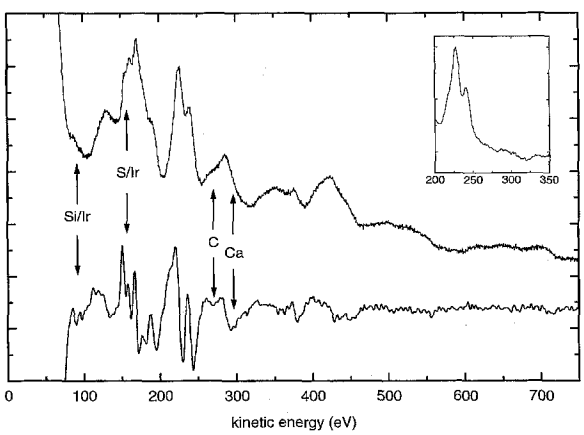

Fig. 3. AE spectra of the Ir(110) surface. The top line represents the energy-spectrum, the bottom line the differentiated $dN(E)/dE$ spectrum for comparison with standard spectra. The positions of possible impurities are marked by arrows. Except for Ca and traces of C, no significant contaminations can be detected. In the inset, the respective energy region without these contaminants, after additional preparation cycles, is shown.

(1–5 K/min) cooling to room temperature. From reflection high-energy electron diffraction (RHEED) measurements during the heating, it is concluded that the formation of features running parallel to the [1$\bar{1}$0] direction starts at approximately 600 ± 50 K because diffuse additional spots appeared above this temperature. In addition, in larger STM images of the c(2 × 2) structure (annealed at 700 K), [1$\bar{1}$0] rows are present first, as can be seen in Fig. 5 discussed above. These findings are consistent with the transition temperatures found by Hetterich et al. [14].

Fig. 7 shows the STM image of a mixed (1 × 3)/(1 × 4) structure. In the image, two types of [1$\bar{1}$0] rows can be seen: thicker and brighter, and thinner and darker. Closer investigation shows that the bright, thick rows correspond to a (1 × 4) period and the thinner, darker rows build a (1 × 3) structure, as can be seen from the height scans along AB and CD in Fig. 8, respectively. The corresponding Fourier transforms of the scans clearly reveal the right distances of 11.5 and 15.4 Å. The brighter, thicker rows are, in fact, double rows separated by one lattice constant, as we conclude from the termination of one of these seen in the marked areas in Fig. 9. This would also explain the height difference (the difference in brightness) between the (1 × 3) rows and the (1 × 4) double rows, i.e. the double rows appear slightly (less than the height of a single step) higher than the single rows because the STM tip cannot resolve them completely and therefore detects a higher electron density. The height difference is therefore only an electronic effect.

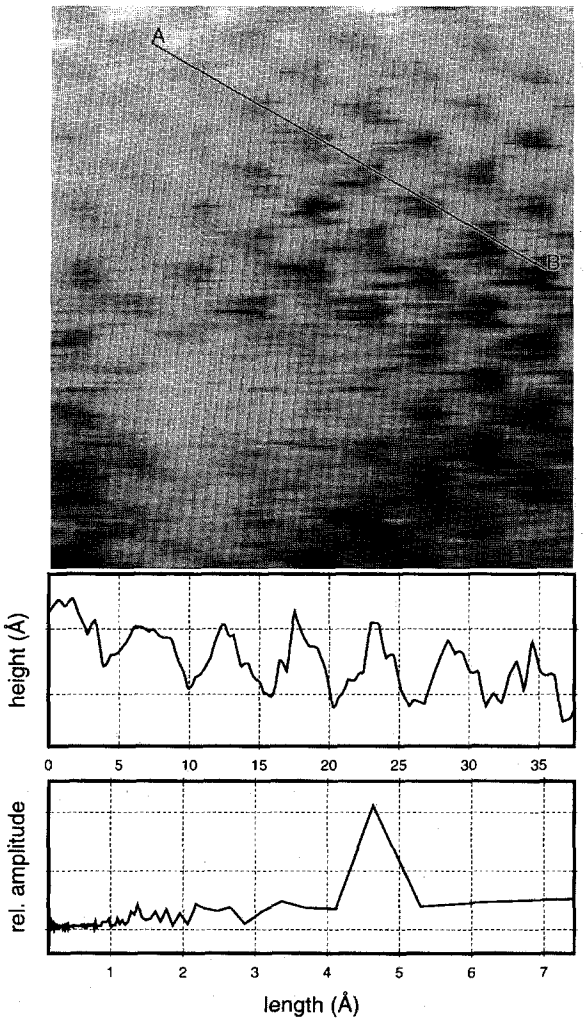

Fig. 4. (38×42) Å^2 STM image of the Ir(110)-c(2×2) structure($U_t=-0.2$ V, $I_t=0.2$ nA). The height scan along AB (upper graph) and its Fourier transform (lower graph) show the period of 4.7 Å.

During our experiments, we observed an increasing tendency of the surface to form the double rows and thereby replacing the $(1\times3)/(1\times4)$ structure by the faceted reconstruction [25]. This tendency is possibly correlated to the Ca contamination. The Ca may cause a "kinetic barrier" in such a way that higher annealing temperatures and/or longer heating times are necessary to obtain the faceted reconstruction, which has been

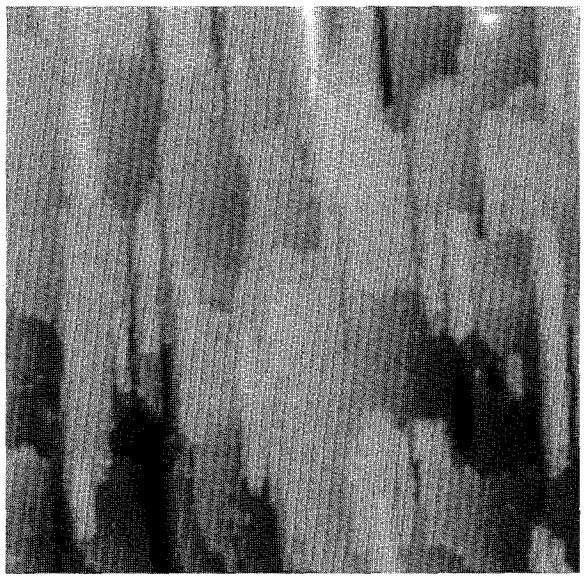

Fig. 5. (500×500) Å^2 STM image of the Ir(110)-c(2×2) structure ($U_t=-0.26$ V, $I_t=0.9$ nA). On each of the small terraces the c(2×2) structure can be found. Note the row-like features at the terrace edges which run parallel to the [1$\bar{1}$0] direction (vertical image axis) and may be the onset of the $(1\times3)/(1\times4)$ formation seen in Fig. 7.

reported previously by Koch et al. [16,17] and Avrin et al. [18].

An LEED pattern of the Ca-contaminated surface is shown in Fig. 10. The LEED pattern observed from this $(1\times3)/(1\times4)$ structure (according to STM) is nearly exactly the same as for the clean, faceted structure. Only occasionally does a slight tendency towards a (1×3) period or a (1×4) period occur where the patterns are less streaky but reveal the same overall intensity distribution. To distinguish in a quantitative manner between these structures, it would be necessary to take LEED $I(V)$ curves, which is not possible with our system.

As was mentioned in almost all studies dealing with the Ir(110) surface, the LEED patterns are "rather complex", "streaked" along the [001] azimuth, and the spots move in a complex manner when varying the energy of the electron-beam. Koch et al. suggested an explanation for this behaviour by superposing the reciprocal lattice of the macroscopic (110) plane with the reciprocal lattice of the (331) facets [16].

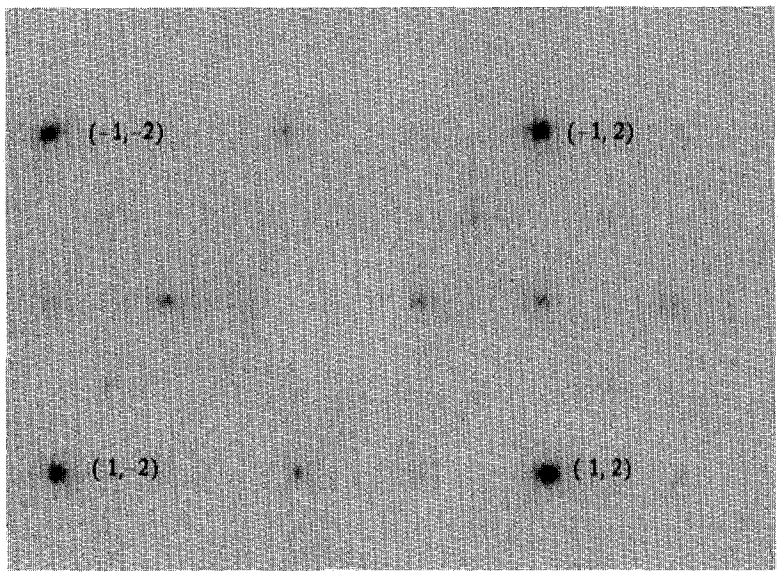

Fig. 6. LEED pattern of the Ir(110)-c(2×2) structure; the electron energy is 146 eV. Several integral-order spots are indexed.

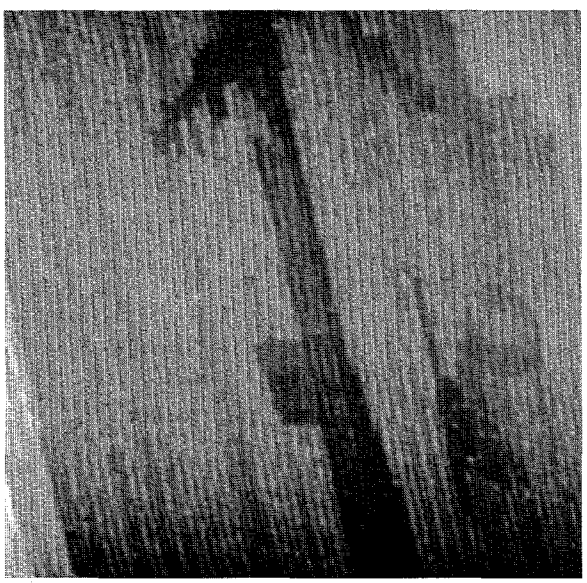

Fig. 7. (1000×1000) Å^2 STM image of the Ir(110)-(1×3)/(1×4) structure ($U_t = -0.28$ V, $I_t = 1.1$ nA). Note there are two types of [1$\bar{1}$0] rows, brighter and thicker ones arid darker and thinner ones. The brighter rows are double rows (see Fig. 9) and are placed $4a_0$ apart (Fig. 8), whereas the darker rows are $3a_0$ apart (Fig. 8).

3. Discussion

We investigated the various structures of the clean Ir(110) surface and the Ir(110) surface with ≈8% Ca with STM, LEED and AES. In agreement with earlier results, the (1×1) structure was prepared via oxygen adsorption, and atomically resolved images revealed ordered [1$\bar{1}$0] rows as was reported in an earlier STM study [17]. The mesoscopic step structure was dominated by many round shaped terraces due to the sputtering and the moderate annealing temperature of 600 K.

The c(2×2) structure has also been atomically resolved in STM images. This has not been yet reported by other groups. The LEED pattern of this structure reveals the same symmetry and indicates a considerably high amount of the structure being present at the surface as the patterns do not change when varying the position of the electron beam on the sample. As the structure has been prepared only with sputtering and slight annealing to 700 K, no oxygen signal was detected in the AE spectra. Thus, it may be questionable as to whether the observed structure is the same as has been reported earlier [8,9,12,20] where the centred spots in the LEED patterns were due to an ordered oxygen overlayer. Further experiments will have

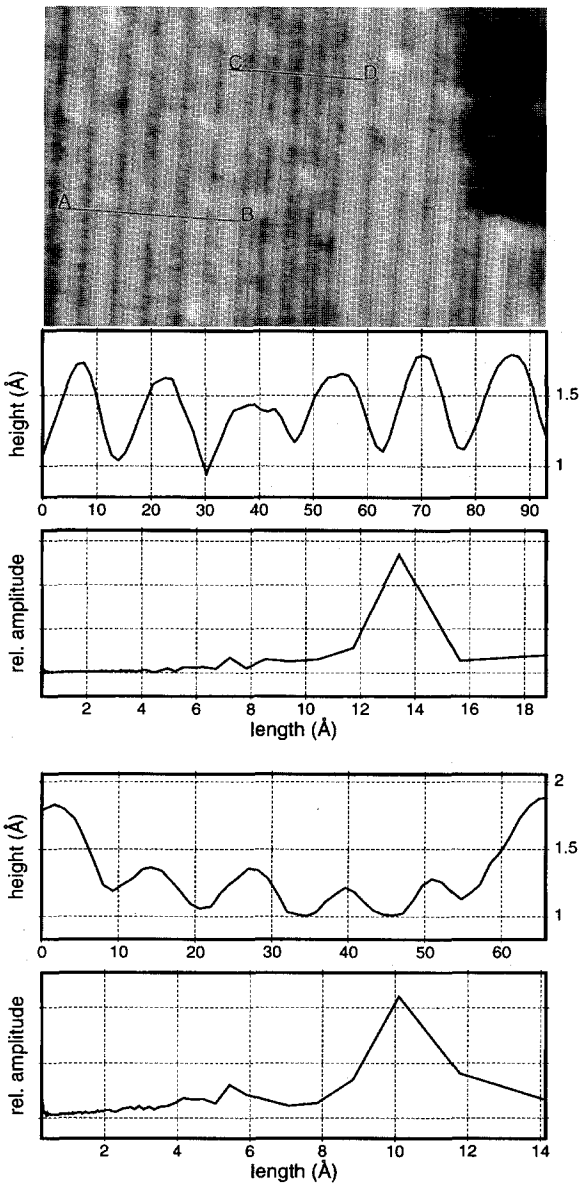

Fig. 8. (150 × 250) Å^2 STM image of the Ir(110)-(1 × 3)/(1 × 4) structure ($U_t = -0.28$ V, $I_t = 1.1$ nA). The height scan along AB (first graph below the image) shows the (1 × 4) part of the surface; the scan along CD (third graph) shows the (1 × 3) part (see also the Fourier transforms which are shown below the respective scans).

to clarify this point. We were succesful in preparing the c(2 × 2) structure in the usual manner via oxygen adsorption, but so far, only LEED data are available.

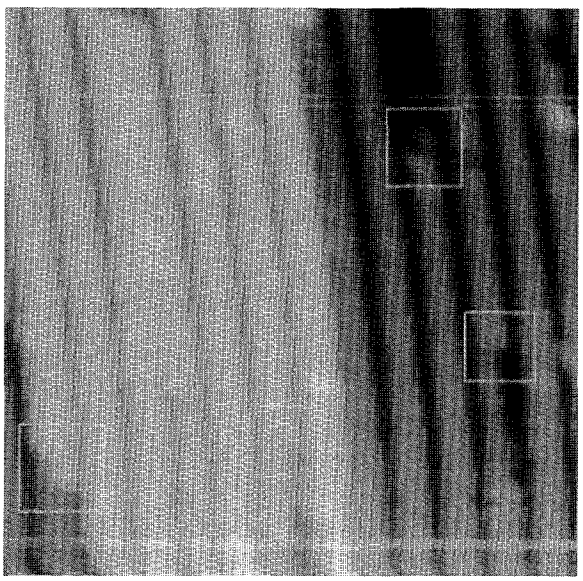

Fig. 9. (200 × 200) Å^2 STM image of the Ir(110)-(1 × 4) structure ($U_t = -0.3$ V, $I_t = 1.0$ nA). In the marked areas, one of the rows forming the double rows terminates. The [1$\bar{1}$0] direction is roughly parallel to the vertical image axis.

The mixed (1 × 3)/(1 × 4) structure on the Ca-contaminated surface has been reported for the first time. It is known from other fcc(110) surfaces (Pt, Au) that Ca tends to enhance the formation of close-packed (111) facets even in very low concentrations [26–28]. Since we never observed large (1 × 3) reconstructed areas in the STM, it is possible that the (1 × 3) reconstruction is influenced by Ca. The double-rows forming the (1 × 4) structure are also seen in quite large amounts on the clean (free of Ca) surface, so this reconstruction seems to be an inherent feature of the ground state of the clean surface. The double rows may represent the first step towards the formation of the (331) facets observed on the clean surface [16–18,25].

Earlier ion-scattering studies favoured a faceted (1 × 3) reconstruction with a considerable amount of unreconstructed (1 × 1) domains [13,15,29]. The size of these domains could not be determined with ion-scattering experiments, so it is possible that the [110] double rows are the (1 × 1) domains observed with ion scattering.

Fig. 11a shows a microscopic model of a

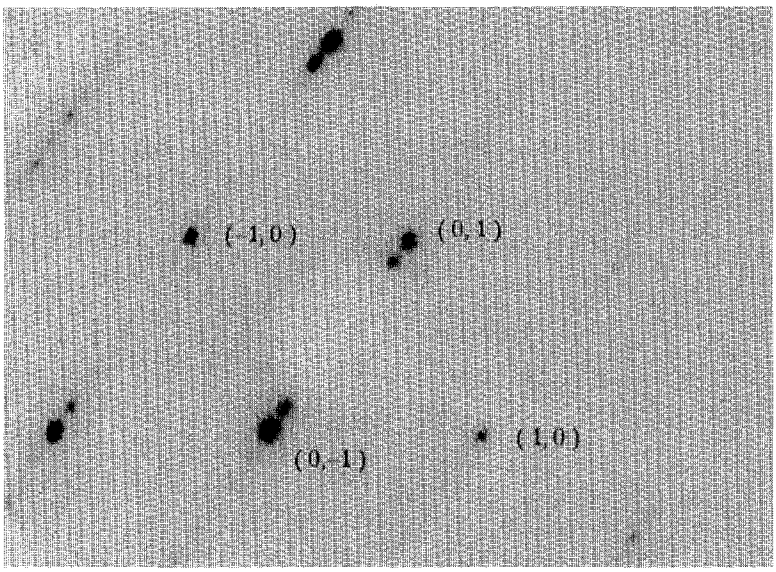

Fig. 10. LEED pattern of the Ir(110)-(1×3)/(1×4)/faceted structure; electron energy, 146 eV. This pattern is mainly (1×4), whereas others are a mixture of (1×3) and (1×4) periodicities (more streaky along the [001] azimuth). The pattern may also be explained by a faceted surface (see text).

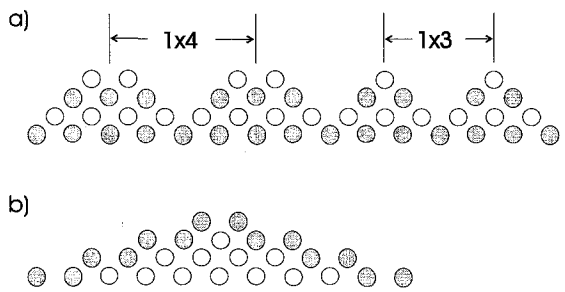

Fig. 11. (a) Model of the (1×3)/(1×4) structure, side view in the [1$\bar{1}$0] direction. The two close-packed rows form a (1×4) period, whereas the neighbouring single rows constitute a (1×3) period. (b) Model of the (331) faceted structure, side view in [1$\bar{1}$0] direction. The shaded atoms indicate the "double-rows" at the sides of the facets and the flat double-row at the top forming a small (1×1) terrace.

(1×3)/(1×4) structure consisting of two double rows lying side by side forming the (1×4) part and neighboured by single rows forming the (1×3) part of the structure. Below (Fig. 11b), a (331) faceted model is shown as proposed by Koch et al. [16]. On top of the structure a close-packed double-row is seen. We note that by placing several double-rows side by side in successively higher layers (shaded atoms in Fig. 11b), a (331) facet is formed automatically.

Acknowledgements

Financial support by the Deutsche Forschungsgemeinschaft (DFG) is greatfully acknowledged.

References

[1] D.G. Fedak, N.A. Gjostein, Acta Metall. 15 (1967) 827.
[2] H.P. Bonzel, R. Ku, J. Vac. Sci. Technol. 9 (1972) 663.
[3] P. Fery, W. Moritz, D. Wolf, Phys. Rev. B 38 (1988) 7275.
[4] E.C. Sowa, M.A. Van Hove, D.L. Adams, Surf. Sci. 199 (1988) 174.
[5] P. Fenter, T. Gustafsson, Phys. Rev. B 38 (1988) 10197.
[6] E. Vlieg, I.K. Robinson, Surf. Sci. 233 (1990) 248–254.
[7] U. Korte, G. Meyer-Ehmsen, Surf. Sci. 271 (1992) 616.
[8] K. Christmann, G. Ertl, Z. Naturforschung 28a (1973) 1144.
[9] J.L. Taylor, W.H. Weinberg, Surf. Sci. 79 (1979) 349.
[10] M.A. Van Hove, W.H. Weinberg, C.-M. Chan, Low-Energy Electron Diffraction, Springer Series in Surface Science 6, Springer, Berlin, 1986.

[11] W. Hetterich, W. Heiland, Surf. Sci. 210 (1989) 129.
[12] H. Bu, M. Shi, F. Masson, J.W. Rabalais, Surf. Sci. Lett. 230 (1990) L140.
[13] H. Bu, M. Shi, J.W. Rabalais, Surf. Sci. 236 (1990) 135.
[14] W. Hetterich, W. Heiland, Surf. Sci. 258 (1991) 307.
[15] C. Höfner, W. Hetterich, H. Niehus, W. Heiland, Nucl. Instrum. Meth. Phys. Res. B 67 (1992) 328.
[16] R. Koch, M. Borbonus, O. Haase, K.H. Rieder, Phys. Rev. Lett. 67 (1991) 3416.
[17] R. Koch, M. Borbonus, O. Haase, K.H. Rieder, Appl. Phys. A 55 (1992) 417.
[18] W.F. Avrin, R.P. Merrill, Surf. Sci. 274 (1992) 231.
[19] C.-M. Chan, S.L. Cunningham, K.L. Luke, W.H. Weinberg, S.P. Withrow, Surf. Sci. 78 (1978) 15.
[20] C.-M. Chan, K.L. Luke, M.A. Van Hove, W.H. Weinberg, S.P. Withrow, Surf. Sci. 78 (1978) 386.
[21] S. Speller, T. Rauch, W. Heiland, Surf. Sci. 342 (1995) 224.
[22] G. Binnig, H. Rohrer, Ch. Gerber, E. Stoll, Surf. Sci. 144 (1984) 321.
[23] T. Michely, G. Comsa, Surf. Sci. 256 (1991) 217.
[24] C.L. Hedberg (Ed.), Handbook of Auger Electron Spectroscopy, Physical Electronics, Inc., 1995.
[25] J. Kuntze, S. Speller, W.H. Heiland, Surf. Sci., to be published.
[26] T. Gritsch, D. Coulman, R.J. Behm, G. Ertl, Surf. Sci. 257 (1991) 297.
[27] R. Michaelis, D.M. Kolb, Surf. Sci. 234 (1990) L281.
[28] M. Stock, J. Risse, U. Korte, G. Meyer-Ehmsen, Surf. Sci. Lett. 233 (1990) L243–L248.
[29] M. Shi, H. Bu, J.W. Rabalais, Phys. Rev. B 42 (1990) 2852.